

IFD: A Large-Scale Benchmark for Insider Filing Violation Detection

Cheng Huang¹, Fan Gao^{1,*}, Yutong Liu^{1,*}, Yadi Liu^{2,3}, Xiaoli Ma⁴, Ye Aung Moe⁵
Yuhan Zhang⁶, Yao Ma⁵, Hao Wang¹, Xiangxiang Wang^{1,†}, Yongbin Yu^{1,†}

¹University of Electronic Science and Technology of China, ²Nanyang Technological University

³Singapore Management University, ⁴Washington State University

⁵University of Nebraska-Lincoln, ⁶University at Buffalo
ybyu@uestc.edu.cn

Abstract

Insider trading violations, particularly delayed disclosures of Form 4 filings, remain a persistent challenge for financial market surveillance. Despite regulatory requirements such as the two-business-day rule of the Securities and Exchange Commission (SEC), enforcement is limited by the lack of large-scale, labeled datasets and task-specific benchmarks. In this paper, we introduce **Insider Filing Delay (IFD)**, the first and largest publicly available dataset for insider disclosure behavior, comprising over one million Form 4 transactions spanning two decades (2002–2025), with structured annotations on delay status, insider roles, governance factors, and firm-level financial indicators. IFD enables the first large-scale formulation of strategic disclosure violation detection as a binary classification task grounded in regulatory compliance. To demonstrate the utility of IFD, we propose **MaBoost**, a hybrid framework, combining a Mamba-based state space encoder with XGBoost, achieving high accuracy and interpretability in identifying high-risk behavioral patterns. Experiments across statistical baselines, deep learning models, and large language models confirm that MaBoost outperforms prior approaches, achieving an F1-score of up to 99.47% under constrained regulatory settings. IFD provides a realistic, reproducible, and behavior-rich benchmark for developing AI models in financial compliance, regulatory forensics, and interpretable time-series classification. All data and codes are available: <https://github.com/CH-YellowOrange/MaBoost-and-IFD>.

Introduction

Ensuring timely and transparent disclosure of insider trading activities is critical to maintaining fairness and efficiency in financial markets. In the United States, the Securities and Exchange Commission (SEC) mandates that corporate insiders must report their trades through Form 4 filings within two business days of execution (Cline and Houston 2023; Wang et al. 2023; Yang et al. 2023). However, strategic delays in disclosure continue to undermine market integrity and investor trust. While prior studies suggest that such delays may be intentional and financially motivated, large-scale empirical analysis remains scarce due to the absence of

high-quality, structured datasets with regulatory-grounded labels (Ma, Ma, and Jiang 2025; Moe and Ma 2024).

To address this gap, we introduce the **Insider Filing Delay (IFD)** dataset, the first large-scale, behavior-rich benchmark specifically curated for detecting delayed insider filings in violation of SEC rules. IFD contains over 4,051,143 Form 4 filings from 2002 to 2025, annotated with binary labels indicating compliance or violation, and enriched with over 50 features, including insider roles, governance structure, market context, and temporal patterns. This dataset enables the formulation of a new AI task: identifying regulatory disclosure violations as a binary classification problem grounded in financial behavior.

To demonstrate the utility of IFD, we develop **MaBoost**, a hybrid framework that combines the sequence modeling capabilities of the Mamba (Gu and Dao 2023; Dao and Gu 2024) state space model with the interpretability of XGBoost (Chen and Guestrin 2016). Our model achieves state-of-the-art performance across multiple benchmarks, significantly outperforming classical statistical models, deep learning baselines, and large language models (LLMs), while offering transparent, interpretable outputs suitable for regulatory auditing.

This paper contributes a realistic, reproducible foundation for AI-based market surveillance and compliance monitoring, and highlights the importance of behavior-aware modeling in financial regulation. All in all, we make the following key contributions:

- We construct IFD, the first and largest publicly available dataset of insider filing behavior, containing over 4,051,143 labeled SEC Form 4 transactions enriched with structured attributes.
- We define a novel binary classification task for detecting strategic disclosure violations, grounded in SEC’s two-day reporting regulation.
- We propose MaBoost, the hybrid model combining Mamba-based sequence encoding with XGBoost classification, achieving high accuracy and interpretability.
- We benchmark IFD across traditional models, deep sequence networks, and LLMs, and show MaBoost consistently outperforms all baselines.

*Equal Contribution; †Corresponding Author

Copyright © 2026, Association for the Advancement of Artificial Intelligence (www.aaai.org). All rights reserved.

Related Work

AI for Finance

Recent advancements in AI for finance have demonstrated promising results in forecasting (Xu et al. 2021; Xu, Wang, and Guo 2021; Yang, Zhang, and Zhang 2020), anomaly detection (Liu et al. 2021; Zhou et al. 2021; Chen et al. 2021), and trading strategy design (Wu et al. 2022; Wang et al. 2023; Araci 2021). Classical models like logistic regression (Hosmer and Lemeshow 2000), XGBoost (Chen and Guestrin 2016), and random forests (Breiman 2001) are widely used for structured financial data. Deep learning models, including RNNs (Elman 1990), LSTMs (Hochreiter and Schmidhuber 1997), and Transformers (Vaswani et al. 2017), have further enhanced sequential pattern recognition for price movements (Wang, Zhang, and Zhao 2022; Feng et al. 2019), sentiment analysis (Zhang, Chen, and Zhao 2020; Liu et al. 2023), and fraud detection (Wang et al. 2022).

Recent works like REST (Xu et al. 2021; Xu, Wang, and Guo 2021) and RSR (Feng et al. 2019; Wang, Zhang, and Zhao 2022) introduce relational modeling for stock trend forecasting, focusing on cross-stock correlations and event propagation (Chung, Rösch, and Zhang 2023). However, these models primarily aim at market-level predictions and often rely on curated or small-scale datasets. In contrast, our work leverages a real-world, large-scale insider trading dataset, IFD, exceeding one million records, enabling richer modeling of behavioral and regulatory signals beyond market movement.

Report Violations Detection

Detection of regulatory violations, such as late filings (Tat-sat and Shater 2025; Wang et al. 2025) or abnormal trade timing (Hsia and Hsu 2024; Liang et al. 2022), remains underexplored in comparison to mainstream financial prediction tasks. Prior studies have treated such violations as outlier detection problems or framed them within rule-based or heuristic systems with limited generalizability (Ding et al. 2015; Yang et al. 2023). While some supervised learning efforts exist, they typically lack sufficient labeled data and fail to capture temporal or contextual nuances in insider behavior (Cline and Houston 2023; Loshchilov and Hutter 2019).

To address these limitations, we propose a novel framework, MaBoost, that not only incorporates temporal and relational structure across trading sequences but also benefits from a uniquely labeled dataset covering a broad spectrum of violation cases (Yang et al. 2023). MaBoost outperforms traditional baselines and aligns with the goals of compliance automation and intelligent regulatory monitoring.

Methodology

MaBoost is designed as a modular, hybrid architecture that combines sequential pattern extraction and structured classification for the detection of insider filing violations. The framework consists of two main components: a Mamba-based sequence encoder and an XGBoost classifier.

Given a historical transaction sequence \mathbf{X}_i , the Mamba sequence encoder processes each time step via a linear state-space mechanism:

$$\mathbf{h}_t = \mathbf{A}_t \mathbf{h}_{t-1} + \mathbf{B}_t \mathbf{x}_i^{(t)}, \quad \mathbf{z}_t = \mathbf{C}_t \mathbf{h}_t \quad (1)$$

The sequence of outputs $\{\mathbf{z}_1, \dots, \mathbf{z}_T\}$ is aggregated into a fixed-length representation \mathbf{h}_i , either by mean pooling or using the final state:

$$\mathbf{h}_i = \text{Aggregate}(\{\mathbf{z}_1, \dots, \mathbf{z}_T\}) \quad (2)$$

The vector \mathbf{h}_i is then passed to an XGBoost classifier composed of M regression trees:

$$\hat{y}_i = f(\mathbf{h}_i) = \sum_{m=1}^M f_m(\mathbf{h}_i) \quad (3)$$

The predicted probability is obtained via sigmoid activation:

$$\hat{p}_i = \sigma(\hat{y}_i) \quad (4)$$

and the final label is determined as:

$$\hat{y}_i^{\text{label}} = \mathbb{I}(\hat{p}_i \geq \tau) \quad (5)$$

The model is trained by minimizing a regularized logistic loss:

$$\mathcal{L} = \sum_{i=1}^n l(y_i, \hat{p}_i) + \sum_{m=1}^M \Omega(f_m) \quad (6)$$

where $l(\cdot)$ is the binary cross-entropy loss and $\Omega(f_m)$ is the complexity regularization term. This formulation allows MaBoost to capture temporal behavioral patterns while retaining interpretable, tree-based decision logic.

As shown in Table 1, all the terms used in this section are summarized below.

Symbol	Description
\mathbf{A}_t	State transition matrix in the Mamba encoder
\mathbf{B}_t	Input projection matrix in the Mamba encoder
\mathbf{C}_t	Output projection matrix in the Mamba encoder
$\mathbf{x}_i^{(t)}$	Feature vector at time t for insider i
\mathbf{X}_i	Historical transaction sequence of insider i
\mathbf{h}_t	Hidden state at time step t in the Mamba encoder
\mathbf{z}_t	Output vector at time t from the Mamba encoder
\mathbf{h}_i	Aggregated behavioral representation of insider i
f	Overall XGBoost classifier function
f_m	The m th decision tree in the XGBoost ensemble
\hat{y}_i	Raw prediction score (logit) for sample i
\hat{p}_i	Predicted probability after sigmoid activation
\hat{y}_i^{label}	Final binary classification label
y_i	Ground-truth label
\mathcal{L}	Overall loss function
$l(y_i, \hat{p}_i)$	Binary cross-entropy loss for sample i
$\Omega(f_m)$	Regularization penalty for the m th tree
$\sigma(\cdot)$	Sigmoid activation function
$\mathbb{I}(\cdot)$	Indicator function for thresholding
τ	Classification threshold (typically 0.5)

Table 1: Key Mathematical Notations in MaBoost

Dataset and Implementation

Dataset

We construct our insider trading dataset by extracting stock transaction records from WRDS¹ and processing them in SAS². Following established standards, we retain trades with valid cleanse codes (R, H, C, L, I), exclude amended filings and option-related transactions, and focus on open market purchases and sales (TRANCODE = P or S) (Cline and Houston 2023). Filings with transaction dates after the report date are removed. To measure reporting delays, we merge the data with an LLM-generated SEC business calendar (2002–2025), incorporating a Python-based two-day filing deadline. Unlike prior work, we preserve trade-level granularity without insider-day aggregation to support machine learning tasks.

IFD Insider Filing Delay contains 4,051,143 transactions, involving over 7,633 firms and 15,573 insiders, covering open market transactions disclosed via Form 4 filings by corporate insiders in U.S. public companies from 2002 to 2025. Among these trades, roughly 17.4% (21,482 transactions) are classified as filing violations, meaning the disclosure occurred after the SEC’s legally mandated deadline, a window reduced to two business days after the Sarbanes-Oxley Act (SOX) in 2002. Filing violations are further categorized based on the length of the delay and the historical behavior of the insider. About 77% of the violations are considered oversight violations, typically delayed by three or fewer business days and committed by insiders who do not frequently violate filing requirements. In contrast, 23% of the violations are deemed intentional violations, characterized by longer delays (≥ 4 business days) and committed by insiders who violate at least 95% of the time.

Role	Total Trades	Violation Rate	Violations
CEO	12,843	10.88%	1,397
Corporate Suite	21,415	10.63%	2,277
Beneficial Owners	18,402	22.24%	4,093
Other Insiders	8,472	16.59%	1,405

Table 2: Insider Roles and Violation Rates

Also, as shown in Table 2, we also looked at different internal roles within the company and their violation rates. Classified statistics on the job titles of employees who violated the rules can help provide a clearer understanding of the approximate proportions when analyzing the motives behind these violations later. This is crucial in determining whether the violation falls under the category of ‘negligent violation’ or ‘intentional violation’.

One sample of IFD has a total of 52 attributes as shown in Table 3. These fields encompass identity information, transaction details, form types, data verification, delays, and adjustments necessary for SEC insider trading reports. Finance experts of our team thoroughly review and check all data, guaranteeing its authenticity and accuracy. The IFD dataset includes six attribute categories: (1) Basic Identification and

Date Information, (2) Company and Security Information, (3) Form and Transaction Details, (4) Transaction Codes and Data Cleansing, (5) Timing and Delay Information, and (6) Additional Fields.

Attribute	Value
DCN	02720220
TRANDATE	08/01/2002
SEQNUM	1
PERSONID	16078646
Owner	SHAVIN HELENE B
Rolecode1	O
Rolecode2	VP
Rolecode3	C
Rolecode4	-
Address1	1 ROCKEFELLER PLAZA
Address2	STE 1430
City	NEW YORK
State	NY
Zipcode	10020
Country	-
Phone	-
Cname	HARRIS & HARRIS GROUP INC
Cnum	H202680000
CUSIP6	413833
CUSIP2	10
Ticker	TINY
SECID	4537
Sector	01
Industry	02
FORMTYPE	4
Acqdisp	A
Optionsell	-
Ownership	D
Sharesheld	500.0000
Sharesheld.Adj	500.0000
Shares	500.0000
Shares.Adj	500.0000
TPRICE	2.79
Tprice.Adj	2.7900
TRANCODE	P
Secitle	COM
Amend	-
Cleanse	R
FDATE	05/29/2012
CDATE	08/07/2002
MAINTDATE	05/27/2012
SECDATE	08/06/2002
SIGDATE	08/06/2002
TRANDATE.AR	08/01/2002
ACQDISP.AR	A
TPRICE.AR	2.79
TRANCODE.AR	P
Gap_Days	-3589
SEC.Business.Day	2002-08-05
SEC.Business.Day_Lag2	2002-08-01
Delay	1
Id	0

Table 3: Details of One Sample of IFD

Basic Identification and Date Information includes DCN (record ID), TRANDATE (transaction date), SEQNUM (record sequence), PERSONID (insider ID), OWNER (insider name), ROLECODE1–4 (insider roles), ADDRESS1/2, CITY, STATE, ZIPCODE, COUNTRY (location details), and PHONE. Company and Security Information covers CNAME (company name), CNUM (internal ID), CUSIP6 and CUSIP2 (issue identifiers), TICKER (stock symbol), SECID (security ID), and classification codes for SECTOR and INDUSTRY. Form and Transaction Details include FORMTYPE (Form 3, 4, 5, or 144), ACQDISP (acquisition ‘A’ or disposition ‘D’), OPTIONSELL (option-related sale flag), and OWNERSHIP (beneficial ownership: Direct or Indirect). SHARES and SHARES_ADJ record transaction volume (raw and adjusted), while SHARESHELD and SHARESHELD_ADJ indicate post-trade holdings. TPRICE

¹<https://wrds-www.wharton.upenn.edu/>

²www.sas.com

and TPRICE_ADJ reflect the transaction price per share (raw and adjusted). Transaction Codes and Data Cleansing contain TRANCODE / TRANCODE_AR (transaction type, e.g., ‘P’ for purchase), SECTITLE (security type), AMEND (amendment flag), and CLEANSE (data confidence level). Timing and Delay Information includes FDATE, CDATE, MAINTDATE (file/create/maintenance dates), SECDATE (SEC receipt date), SIGDATE (signature date), and TRAN-DATE_AR / ACQDISP_AR / TPRICE_AR (as-reported values). gap_days measures transaction-to-filing delay. SEC_Business_Day and SEC_Business_Day_Lag2 mark filing timeliness, while delay quantifies reporting lag in days. Additional Fields include the Rule 10b5-1 flag (plan-based trade), Market Value of Transaction (Form 144 estimate), and Proposed Number of Shares (expected to be sold under Form 144). Id is the internal unique identifier for the record, which is the label (1 means illegal operation). For the Table 3, - means none.

All in all, IFD can be used to analyze insider trading behavior, filing violations, market reactions, corporate governance, regulatory effectiveness, and firm performance, providing valuable insights into the dynamics of insider compliance and its impact on financial markets. Other important information can be found in Supplementary Material.

Implementation

Hyperparameter Table 4 summarizes the hyperparameter configurations used for training the MaBoost framework, which integrates the Mamba state space encoder with an XGBoost classifier. For the Mamba module, we adopt a lightweight sequence encoder with bidirectional modeling and GELU activation (Hendrycks and Gimpel 2016). For XGBoost, we apply standard configurations suitable for imbalanced binary classification tasks, with regularization and subsampling strategies. This configuration balances model capacity, interpretability, and computational efficiency, and performs robustly across all evaluation scenarios. The training epoch is 200 and the validation is done by ten-fold cross validation.

Mamba		XGBoost	
Perparameter	Value	Perparameter	Value
d_model	256	objective	binary_logistic
n_layers	4	tree_method	hist
ssm_rank	4	max_depth	10
dropout	0.1	min_child_weight	10
activation	GELU	gamma	0.8
pre_norm	True	subsample	0.8
use_bidirectional	True	colsample_bytree	0.8
seq_len	100	learning_rate	0.1
bias	True	n_estimators	3000
norm_epsilon	0.00005	reg_alpha	0.1
tuning_strategy	Optuna	reg_lambda	1.0

Table 4: Hyperparameter Settings for MaBoost

Hardware The hardware specifications for training and testing include 4 4090-Ti GPUs ($4 \times 24\text{GB}$), 64GB of RAM, 8 CPU cores per node, and a total of 6 nodes.

Experimental Result

Experimental Setup

For the IFD dataset, input features can be configured in three modes: (1) Equal Weight; (2) Constraint Condition; (3) Suspected Violation. In the *Equal Weight* setting, all 52 attributes are treated uniformly, providing a baseline to evaluate the model’s capacity for pattern extraction without prior assumptions. The *Constraint Condition* setting incorporates empirical insights by downplaying feature groups with limited standalone impact (e.g., *Spatiotemporal* (Cline and Houston 2023)). MaBoost’s adaptive weighting compensates by capturing their interactions with stronger signals. The *Suspected Violation* setting focuses on subtle behavioral cues such as trading history or delayed filings that gain importance when aligned with abnormal financial patterns. MaBoost’s co-attentive design effectively amplifies such weak but correlated indicators, leading to substantial improvements in precision and recall. This underscores the importance of retaining diverse features for reliable detection of nuanced violations (Moe and Ma 2024).

We evaluate experimental results using Recall, Precision, and F1-Score, which are standard metrics for binary classification tasks ($\times 100\%$). We highlight the best-performing value in bold and the second-best in underline. The training epoch is 500 and the validation is done by ten-fold cross validation.

Baseline Model We choose these following methods or models: Linear Regression (Montgomery, Peck, and Vining 2012), Logistic Regression (Hosmer and Lemeshow 2000), Seq2Seq (Sutskever, Vinyals, and Le 2014), RNN (Elman 1990), Bi-RNN (Schuster and Paliwal 1997), LSTM (Hochreiter and Schmidhuber 1997), Bi-LSTM (Graves and Schmidhuber 2005), GRU (Cho et al. 2014), Transformer (Vaswani et al. 2017), Mamba (Gu and Dao 2023), Decision Tree (Breiman et al. 1984), Random Forest (Breiman 2001), XGBoost (Chen and Guestrin 2016), BERT (Devlin et al. 2019; Liu et al. 2025a), CINO (Zhou et al. 2022) and RoBERTa (Liu et al. 2019, 2025b). We also conducted comparative experiments using a set of encoder-decoder frameworks, including combinations of CNN (LeCun et al. 1998) (ResNet-152 (He et al. 2016)), Vision Transformer (ViT) (Dosovitskiy et al. 2020), and Convolutional Vision Transformer (ConViT) (d’Ascoli et al. 2021) encoders with various decoders (e.g., RNN (Elman 1990), LSTM (Hochreiter and Schmidhuber 1997), Transformer (Vaswani et al. 2017) and Mamba (Gu and Dao 2023)). For parameter optimization, we selected tool Optuna³ as the optimization method.

Large Language Model We also evaluate several LLMs, categorized as open-source and closed-source. Open-source models include the LLaMA (Touvron et al. 2023a,b; Team and AI 2024), Qwen (Bai et al. 2023; Team and Cloud 2024a,b, 2025), and DeepSeek (DeepSeek-AI et al. 2024, 2025) families, while closed-source models include GPT (Brown et al. 2020; OpenAI 2024), Claude (Anthropic 2024), and Gemini (Anil et al. 2023). For open-source

³<https://optuna.org/>

LLM	Version	Prompt-based N-shot			Embedding-based Classification			Fine-tuning with the Classification Head							
		Temp	Top_p	Stream	Dim Change	Method	Classifier	Optimizer	LR	DR	GC	HS	BS	MSL	Epoch
GPT	3.5-Turbo	1.0	1.0	False	1536→1024	TC	MLP	AdamW	10^{-5}	0.1	1.0	256	8	512	5
	4O	1.0	1.0	False	1536→1024	TC	MLP	AdamW	10^{-5}	0.1	1.0	256	8	512	5
	O1-mini	1.0	1.0	True	1536→1024	TC	MLP	AdamW	10^{-5}	0.1	1.0	256	8	512	5
	O1	1.0	1.0	True	1536→1024	TC	MLP	AdamW	10^{-5}	0.1	1.0	256	8	512	5
LlaMA	3.1-405B	0.6	0.9	False	4096→1024	PCA	MLP	AdamW	10^{-5}	0.1	1.0	256	8	512	5
	3.1-70B	0.6	0.9	False	4096→1024	PCA	MLP	AdamW	10^{-5}	0.1	1.0	256	8	512	5
	3.1-8B	0.6	0.9	False	4096→1024	PCA	MLP	AdamW	10^{-5}	0.1	1.0	256	8	512	5
Qwen	2.5-72b	0.7	0.8	False	4096→1024	LP	MLP	AdamW	10^{-5}	0.1	1.0	256	8	512	5
	2.5-32b	0.7	0.8	False	4096→1024	LP	MLP	AdamW	10^{-5}	0.1	1.0	256	8	512	5
	2.5-7b	0.7	0.8	False	4096→1024	LP	MLP	AdamW	10^{-5}	0.1	1.0	256	8	512	5
DeepSeek	R1	1.0	None	True	4096→1024	MP+PCA	MLP	AdamW	10^{-5}	0.1	1.0	256	8	512	5
	V3	1.0	None	False	4096→1024	MP+PCA	MLP	AdamW	10^{-5}	0.1	1.0	256	8	512	5
Claude Gemini	3.5-Sonnet	1.0	None	False	1024	-	MLP	AdamW	10^{-5}	0.1	1.0	256	8	512	5
	1.5-Flash	None	0.95	False	3072→1024	TC 1024	MLP	AdamW	10^{-5}	0.1	1.0	256	8	512	5

Table 5: Hyperparameters Setting of LLMs

models, we evaluate the Qwen-2.5 (2.5-7B, 2.5-32B, 2.5-72B) and DeepSeek families via their official APIs, and the LLaMA (3.1-8B, 3.1-70B, 3.1-405B) family through the LLaMA-API platform. Closed-source models are similarly evaluated through their respective official APIs. These evaluation details will be fully documented in the final version to ensure transparency and reproducibility.

We evaluate the IFD dataset using three classification paradigms based on LLMs: (1) Prompt-based Zero/Few-shot Inference; (2) Embedding-based Classification; (3) Fine-tuning with the Classification Head.

Table 5 presents the hyperparameters for prompt-based zero-shot and few-shot classification. In this setting, LLMs are guided by natural language prompts to generate classification labels without additional training. For embedding-based classification, LLMs act as frozen feature extractors, producing contextual embeddings from hidden states. These embeddings are then passed to an external binary classifier, ensuring efficiency and flexibility across tasks. To ensure fair comparison, all embeddings are projected to 1024 dimensions using PCA (Jolliffe 1986; Pedregosa et al. 2011), linear projection (Jolliffe 1986; Vaswani et al. 2017), mean pooling (Reimers and Gurevych 2019; Hamilton, Ying, and Leskovec 2017), and truncation (Vaswani et al. 2017; OpenAI 2024). The classifier is a two-layer MLP (Rumelhart, Hinton, and Williams 1986). In the fine-tuning setup, a classification head (also an MLP (Rumelhart, Hinton, and Williams 1986)) is trained jointly with the LLM for binary classification, enabling task-specific representation learning. This approach typically achieves higher accuracy but at the cost of increased computation and potential overfitting. Cross-entropy loss (Mao, Mohri, and Zhong 2023) is used, with cosine decay and 10% warm-up, and optimization is performed using AdamW (Loshchilov and Hutter 2019).

Note: Temperature = Temp; Linear Projection = LP; Mean Pooling = MP; Truncate = TC; Learning Rate = LR; Dropout Rate = DR; Gradient Clipping = GC; Hidden Size = HS; Batch Size = BS; Max Sequence Length = MSL.

Comparative Experiment

Baseline Model Table 6 presents the performance comparison of various models across three input configurations on the IFD dataset. Among all models, MaBoost consistently achieves the best performance across all three input types, significantly outperforming baselines in terms of F1-Score. Notably, MaBoost demonstrates strong stability, with Recall, Precision, and F1-Score remaining closely aligned and exhibiting no significant fluctuations, indicating balanced decision boundaries and robust generalization. Transformer-based hybrids (e.g., ConViT-Transformer and ConViT-Mamba) also show competitive results, particularly under the *Constraint Condition* and *Suspected Violation* settings. Traditional models such as Logistic Regression and XGBoost perform reasonably well but fall short in capturing complex interaction patterns.

Large Language Model As shown in Figure 1, although LLMs have shown remarkable capabilities in natural language understanding, their performance on structured financial datasets like IFD remains significantly limited. This is primarily due to three factors: (1) LLMs are not optimized for tabular data reasoning, which involves numerical patterns and relational attributes rather than textual semantics; (2) they are prone to overfitting when the task lacks sufficient labeled context for in-context learning; and (3) zero-shot and few-shot prompting underperform due to the semantic gap between instruction-style prompts and highly structured features. This observation underscores the necessity of tailored AI models in compliance-critical financial domains, rather than relying on general-purpose LLMs.

Figure 2 presents the embedding-based classification performance of various LLMs on the IFD. Among all LLMs, GPT-4O and LLaMA-3.1-405B consistently achieve strong results, with GPT-4O obtaining the highest F1-Score under Equal Weight and Suspected Violation tasks. In contrast, smaller-scale models such as Qwen-2.5-7b and GPT-O1-mini exhibit relatively lower performance across all settings. The inclusion of constraint-based logic notably improves most models’ precision, recall, and F1 scores, highlighting the benefits of incorporating domain-specific knowledge

Model	Equal Weight			Constraint Condition			Suspected Violation		
	Precision	Recall	F1-Score	Precision	Recall	F1-Score	Precision	Recall	F1-Score
Linear Regression	52.39	12.54	20.24	76.15	14.42	24.25	67.79	13.72	22.75
Logistic Regression	59.89	34.24	42.18	85.60	57.07	60.79	69.72	41.75	45.98
Seq2Seq	76.67	74.68	77.02	93.97	94.85	93.15	92.38	93.14	92.89
RNN	77.01	77.56	78.07	90.36	94.27	91.51	78.98	79.97	81.24
Bi-RNN	81.19	84.27	83.39	93.97	94.85	93.15	90.27	91.69	90.89
LSTM	78.58	79.42	79.23	90.24	94.28	91.50	84.87	86.65	85.93
Bi-LSTM	83.37	85.13	84.29	95.05	99.73	97.33	91.28	92.97	92.09
GRU	82.19	83.27	83.09	88.88	94.28	89.15	84.19	86.07	85.74
Transformer	87.32	87.98	87.07	96.71	<u>99.81</u>	98.29	91.17	68.94	71.28
Mamba	86.98	87.27	87.15	98.23	98.74	<u>98.69</u>	<u>93.59</u>	94.27	93.89
Decision Tree	77.86	54.98	61.21	96.66	44.08	<u>60.55</u>	81.92	83.57	82.62
Random Forest	79.86	82.98	83.27	93.17	94.60	92.88	86.17	80.93	76.84
XGBoost	88.71	90.03	90.17	97.91	97.87	97.65	91.21	90.17	87.28
BERT	91.37	<u>92.44</u>	<u>91.89</u>	97.98	97.97	97.78	92.31	92.92	91.23
CINO	90.34	91.09	90.87	97.25	84.85	90.63	88.97	89.91	89.37
RoBERTa	<u>92.32</u>	91.12	90.89	97.03	78.97	87.07	93.05	<u>94.75</u>	<u>93.98</u>
CNN-Seq2Seq	81.23	82.17	81.98	96.66	44.08	60.65	92.38	89.17	86.18
CNN-RNN	82.47	83.18	83.05	95.29	66.76	73.79	91.42	72.39	79.69
CNN-LSTM	81.39	82.73	82.07	95.98	95.95	94.23	77.65	56.42	62.27
CNN-GRU	82.13	84.38	82.45	96.69	71.99	79.42	85.91	87.53	86.29
ViT-RNN	84.49	83.18	71.49	97.30	75.99	85.34	87.27	72.72	78.26
ViT-LSTM	86.53	89.41	87.87	97.88	89.41	93.18	88.91	92.57	90.14
ViT-Transformer	89.96	92.35	91.84	97.98	97.99	<u>97.81</u>	89.98	47.91	58.95
ViT-Mamba	87.44	89.71	90.37	98.24	93.72	95.85	90.37	83.62	84.13
ConViT- RNN	87.98	89.31	88.79	95.94	98.95	97.20	91.07	92.16	91.79
ConViT-LSTM	89.03	91.27	90.76	96.36	65.09	71.99	92.78	78.94	82.16
ConViT-Transformer	<u>93.16</u>	<u>93.98</u>	92.07	94.28	<u>98.97</u>	97.05	93.47	<u>95.19</u>	<u>94.87</u>
ConViT-Mamba	92.28	93.34	<u>92.89</u>	<u>98.64</u>	91.32	94.36	<u>94.16</u>	89.79	90.39
MaBoost	94.93	95.48	94.79	99.09	99.85	99.47	96.24	97.08	96.76

Table 6: Comparative Experiment Among Models on IFD

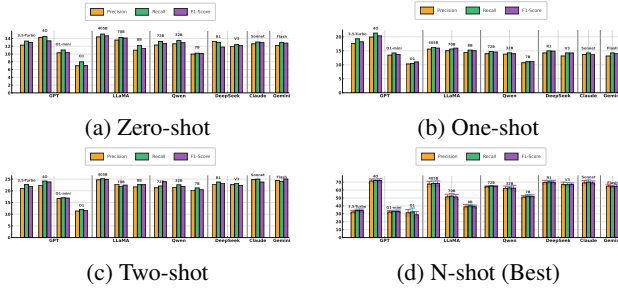


Figure 1: Prompt-based N-shot Experiment of LLMs on IFD

into the classification process.

Figure 3 reports the full fine-tuning results of various LLMs on the IFD dataset using a unified MLP classification head. GPT-4O and LLaMA-3 405B consistently outperform others, with GPT-4O achieving the highest F1-score (87.44) under Equal Weight and LLaMA-3 405B reaching 90.67 under Constraint Condition. DeepSeek-V3 shows notable strength in Suspected Violation detection (F1: 89.13), while smaller models such as GPT-3.5, Qwen-2.5-7B, and LLaMA-3.1-8B perform comparatively lower. Claude and Gemini maintain stable performance.

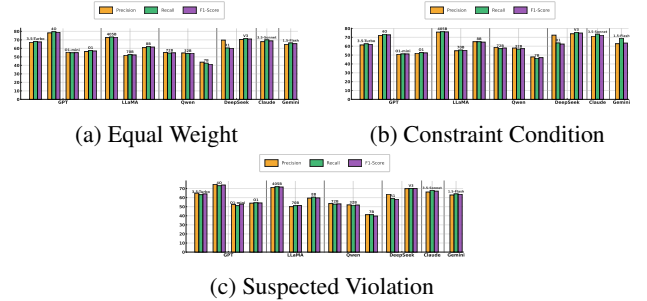


Figure 2: Embedding-based Classification of LLMs On IFD

Compared with LLMs, MaBoost outperforms all across all settings, demonstrating its superiority in regulatory classification tasks and highlighting the strong discriminatory capability of the IFD dataset, enabling comprehensive evaluation and comparison among state-of-the-art models.

Ablation Experiment

IFD To assess the value of each feature group in MaBoost, we conduct an ablation study by removing individual categories, as detailed in Table 7. Performance drops with the exclusion of any group, confirming their comple-

Feature Removed	Equal Weight			Constraint Condition			Suspected Violation		
	Precision	Recall	F1-Score	Precision	Recall	F1-Score	Precision	Recall	F1-Score
Insider History (InsiderRatio, FirmRatio)	88.14	89.57	86.09	95.38	96.82	95.79	91.37	92.41	91.76
Trade Characteristics (TradeValue, Delay)	91.02	91.76	91.33	96.57	90.35	96.92	82.65	84.07	83.21
Governance (BlockholderRatio, HHI)	92.53	92.62	92.11	87.22	87.91	87.52	73.18	75.01	74.06
Financial Health (ROA, Leverage, Tobin's Q)	93.71	93.85	93.71	98.36	99.08	98.65	84.81	85.72	85.09
Spatiotemporal (Ln(Distance), Gap Days)	92.89	92.41	82.33	87.74	88.46	77.98	64.16	65.47	64.79
Full Dataset	94.93	95.48	94.79	99.09	99.85	99.47	96.24	97.08	96.76

Table 7: Ablation Experiment on IFD Feature Groups with MaBoost

Model	Equal Weight			Constraint Condition			Suspected Violation		
	Precision	Recall	F1-Score	Precision	Recall	F1-Score	Precision	Recall	F1-Score
Decision Tree	77.86	54.98	61.21	96.66	44.08	60.55	81.92	83.57	82.62
+ Transformer	81.74	62.37	68.64	97.34	48.12	63.67	83.68	85.33	84.49
+ Mamba	84.09	66.24	72.72	97.89	50.71	66.12	85.94	87.85	86.73
Random Forest	79.86	82.98	83.27	93.17	94.60	92.88	86.17	80.93	76.84
+ Transformer	83.92	85.33	84.60	96.23	96.94	96.32	87.88	84.21	80.52
+ Mamba	86.30	87.95	87.01	97.02	97.76	97.23	90.23	86.15	82.79
XGBoost	88.71	90.03	90.17	97.91	97.87	97.65	91.21	90.17	87.28
+ Transformer	91.24	92.35	91.79	98.16	98.92	98.51	93.14	94.01	93.52
Mamba	86.98	87.27	87.15	98.23	98.74	98.69	93.59	94.27	93.89
+ NoConv	84.33	84.87	84.60	97.03	97.64	97.31	91.45	92.03	91.71
+ NoRes	83.27	83.91	83.58	96.82	96.93	96.73	90.83	91.27	91.04
+ d8	85.42	85.63	85.49	97.36	97.88	97.55	92.03	92.86	92.44
+ dt1	85.76	86.07	85.92	97.68	98.04	97.85	92.28	93.04	92.66
+ GELU	85.91	86.38	86.14	97.52	98.02	97.77	92.74	93.55	93.14
MaBoost	94.93	95.48	94.79	99.09	99.85	99.47	96.24	97.08	96.76

Table 8: Ablation Experiment of MaBoost

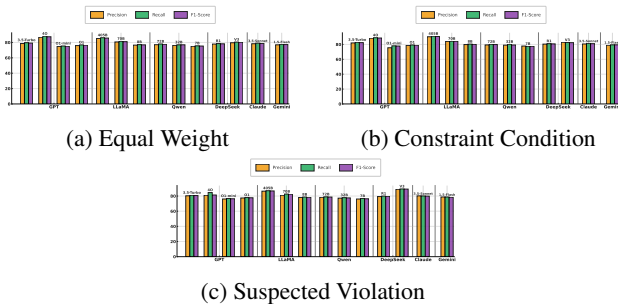


Figure 3: Full Fine-tuning Performance of LLMs on IFD

mentary roles. Notably, removing **Insider History** or **Spatiotemporal** features under the *Suspected Violation* setting leads to a marked decrease in F1-score, underscoring their central importance for violation detection. In contrast, *Financial Health* and *Governance* features are more influential in the *Equal Weight* and *Constraint Condition* scenarios. These results highlight the necessity of a comprehensive feature set for robust violation identification.

MaBoost To assess the impact of different modules and design choices in MaBoost, we conduct ablation studies on three base classifiers, Decision Tree, Random Forest, and

XGBoost, progressively augmenting them with Transformer and Mamba backbones, as shown in Table 8. Adding a Transformer consistently improves decision boundary learning, while replacing it with Mamba yields further gains, reflecting Mamba’s superior ability to model long-range dependencies in tabular data. We further analyze the Mamba backbone through controlled variants. Key Mamba components include state dimension, time interpolation, convolutional input projection, gating and normalization strategies, and activation function. Removing the convolutional projection or residual connections significantly reduces performance, underscoring their roles in spatial encoding and stable optimization. Varying the state dimension or time step resolution provides marginal improvements, while switching the activation from SiLU to GELU slightly degrades results, indicating better alignment of Mamba’s default activation with its architecture. Collectively, these ablations confirm that each architectural element is essential to Mamba’s effectiveness, driving both the robustness and generalization of MaBoost in complex rule-based classification tasks.

Conclusion

This paper’s primary contribution is the introduction of the IFD dataset, a comprehensive, regulatory-grade benchmark for insider filing violation detection. Constructed from authentic SEC EDGAR filings and detailed financial records,

IFD comprises 52 meticulously selected features, covering insider trading history, corporate governance, transaction metadata, temporal context, and firm-level health indicators. IFD provides unparalleled granularity and legal traceability, enabling rigorous empirical research and real-world compliance applications. Its design aligns with regulatory realities, bridging the gap between legal reasoning and machine learning, and supporting both high predictive accuracy and interpretability required for auditing and supervision. Building on IFD, we further propose MaBoost, a hybrid boosting framework that leverages adaptive weighting and neural attention to fully exploit the dataset’s rich structure. Extensive experiments show that the combination of IFD and MaBoost delivers significant performance gains over traditional models and large language models across various evaluation settings, underscoring the dataset’s value as a foundation for future advances in regulatory AI.

Future Work

In future work, we aim to (1) expand the IFD dataset to cover international jurisdictions and multilingual filings; (2) incorporate unstructured textual disclosures (e.g., Form 10-K narratives) using document-level embeddings; and (3) explore causal learning frameworks to uncover deeper compliance logic beyond statistical correlation, facilitating proactive regulatory interventions.

Acknowledgement

This work was supported in part by the National Science and Technology Major Project under Grant 2022ZD0116100, in part by the Sichuan Provincial Major Science and Technology Project under Grant 2024ZDZX0012, in part by the National Natural Science Foundation of China under Grants 62276055 and 62406062, in part by the Sichuan Science and Technology Program under Grant 2023YFG0288, and in part by the Natural Science Foundation of Sichuan Province under Grant 2024NSFSC1476.

References

Anil, R.; Dai, A. M.; Firat, O.; Johnson, M.; Lepikhin, D.; Passos, A.; Shakeri, S.; Taropa, E.; Bailey, P.; Chen, Z.; Shazeer, N.; et al. 2023. Gemini 1: 2 Trillion Token Multimodal Models with Fast Training and Inference. *arXiv preprint arXiv:2312.11805*.

Anthropic. 2024. Claude 3 Family of Language Models. <https://www.anthropic.com/news/claude-3-family>. Accessed July 2025.

Araci, D. 2021. SFinBERT: A Pretrained Language Model for Financial Services. In *Proceedings of the 2nd Workshop on Financial Technology and Natural Language Processing (FinNLP)*, 1–9.

Bai, J.; Bai, S.; Yang, Y.; Wang, T.; Wang, T.; Jiang, J.; Ren, X.; Liu, J.; Liu, H.; Zhu, W.; Song, L.; Zhao, W. X.; and Zhu, J. 2023. Qwen Technical Report. *arXiv preprint arXiv:2309.16609*.

Breiman, L. 2001. Random Forests. *Machine Learning*, 45(1): 5–32.

Breiman, L.; Friedman, J.; Olshen, R. A.; and Stone, C. J. 1984. *Classification and Regression Trees*. Wadsworth International Group.

Brown, T. B.; Mann, B.; Ryder, N.; Subbiah, M.; Kaplan, J.; Dhariwal, P.; Neelakantan, A.; Shyam, P.; Sastry, G.; Askell, A.; Agarwal, S.; Herbert-Voss, A.; Krueger, G.; Henighan, T.; Child, R.; Ramesh, A.; Ziegler, D.; Wu, J.; Winter, C.; Hesse, C.; Chen, M.; Sigler, E.; Litwin, M.; Gray, S.; Chess, B.; Clark, J.; Berner, C.; McCandlish, S.; Radford, A.; Sutskever, I.; and Amodei, D. 2020. Language Models are Few-Shot Learners. In *Proceedings of the 34th Conference on Neural Information Processing Systems (NeurIPS)*.

Chen, T.; and Guestrin, C. 2016. XGBoost: A scalable tree boosting system. In *Proceedings of the 22nd ACM SIGKDD International Conference on Knowledge Discovery and Data Mining*, 785–794. ACM.

Chen, Y.; Xu, C.; Zhao, W. X.; Liu, J.; Liu, W.; Du, X.; and Zhang, R. 2021. HiRN: Hierarchical Relational Networks for Stock Price Movement Prediction. In *Proceedings of the AAAI Conference on Artificial Intelligence*, volume 35, 4020–4027.

Cho, K.; Van Merriënboer, B.; Bahdanau, D.; and Bengio, Y. 2014. Learning Phrase Representations using RNN Encoder–Decoder for Statistical Machine Translation. *arXiv preprint arXiv:1406.1078*.

Chung, K. H.; Rösch, D.; and Zhang, Y. 2023. Competition and Execution Quality in the Market for Retail Trading. Working Paper 4669930, SSRN Electronic Journal. December 19, 2023.

Cline, B. N.; and Houston, C. 2023. Insider Filing Violations and Illegal Information Delay. *Journal of Financial and Quantitative Analysis*, 58(5): 2262–2297.

Dao, T.; and Gu, A. 2024. Transformers are SSMs: Generalized Models and Efficient Algorithms Through Structured State Space Duality. In *International Conference on Machine Learning (ICML)*.

d’Ascoli, S.; Touvron, H.; Leavitt, M.; Morcos, A.; Biroli, G.; and Sagun, L. 2021. ConViT: Improving Vision Transformers with Soft Convolutional Inductive Biases. In *Proceedings of the 38th International Conference on Machine Learning (ICML)*, 2286–2296.

DeepSeek-AI; Guo, D.; Luo, F.; Wang, B.; . . . ; and Yang, X. 2025. DeepSeek-R1: A Reasoning-Oriented LLM Trained via Reinforcement Learning and Distillation. *arXiv preprint arXiv:2501.12948*.

DeepSeek-AI; Liu, A.; Feng, B.; Lu, C.; . . . ; and Pan, Z. 2024. DeepSeek-V3: A Mixture-of-Experts LLM with 671B Parameters (37B Active) and Efficient Training. *arXiv preprint arXiv:2412.19437*.

Devlin, J.; Chang, M.-W.; Lee, K.; and Toutanova, K. 2019. BERT: Pre-training of Deep Bidirectional Transformers for Language Understanding. In *Proceedings of the 2019 Conference of the North American Chapter of the Association for Computational Linguistics: Human Language Technologies*, 4171–4186. Association for Computational Linguistics.

- Ding, X.; Zhang, Y.; Liu, T.; and Duan, J. 2015. Deep Learning for Event-Driven Stock Prediction. In *Proceedings of the International Joint Conference on Artificial Intelligence (IJCAI)*, 2327–2333.
- Dosovitskiy, A.; Beyer, L.; Kolesnikov, A.; Weissenborn, D.; Zhai, X.; Unterthiner, T.; Dehghani, M.; Minderer, M.; Heigold, G.; Gelly, S.; Uszkoreit, J.; and Houlsby, N. 2020. An Image is Worth 16x16 Words: Transformers for Image Recognition at Scale. *arXiv preprint arXiv:2010.11929*.
- Elman, J. L. 1990. Finding structure in time. *Cognitive Science*, 14(2): 179–211.
- Feng, F.; Liu, H.; Lv, Y.; Zhang, W.; Zheng, K.; and He, X. 2019. Temporal Relational Ranking for Stock Prediction. *ACM Transactions on Information Systems (TOIS)*, 38(2): 1–30.
- Graves, A.; and Schmidhuber, J. 2005. Framewise phoneme classification with bidirectional LSTM and other neural network architectures. In *Proceedings of the IEEE International Joint Conference on Neural Networks (IJCNN)*, 2047–2052. IEEE.
- Gu, A.; and Dao, T. 2023. Mamba: Linear-Time Sequence Modeling with Selective State Spaces. *arXiv preprint arXiv:2312.00752*.
- Hamilton, W. L.; Ying, R.; and Leskovec, J. 2017. Inductive Representation Learning on Large Graphs. In *Proc. NeurIPS*, 1025–1035.
- He, K.; Zhang, X.; Ren, S.; and Sun, J. 2016. Deep Residual Learning for Image Recognition. In *Proceedings of the IEEE Conference on Computer Vision and Pattern Recognition (CVPR)*, 770–778.
- Hendrycks, D.; and Gimpel, K. 2016. Gaussian Error Linear Units (GELUs). *arXiv preprint arXiv:1606.08415*.
- Hochreiter, S.; and Schmidhuber, J. 1997. Long short-term memory. *Neural Computation*, 9(8): 1735–1780.
- Hosmer, D. W.; and Lemeshow, S. 2000. *Applied Logistic Regression*. John Wiley & Sons, 2nd edition.
- Hsia, S.-C.; and Hsu, C.-Y. 2024. Real-Time Monitor and Control System for Abnormal Motor Vibrations. *IEEE Transactions on Instrumentation and Measurement*, 73: 1–11.
- Jolliffe, I. T. 1986. Principal Component Analysis. *Springer Series in Statistics*.
- LeCun, Y.; Bottou, L.; Bengio, Y.; and Haffner, P. 1998. Gradient-based learning applied to document recognition. *Proceedings of the IEEE*, 86(11): 2278–2324.
- Liang, H.; Song, L.; Du, J.; Li, X.; and Guo, L. 2022. Consistent Anomaly Detection and Localization of Multivariate Time Series via Cross-Correlation Graph-Based Encoder–Decoder GAN. *IEEE Transactions on Instrumentation and Measurement*, 71: 1–10.
- Liu, X.-Y.; Wang, B.; Liu, Y.; and Yang, X.-Y. 2021. FinRL: Deep Reinforcement Learning Framework to Automate Trading in Quantitative Finance. *arXiv preprint arXiv:2011.09607*.
- Liu, Y.; Ott, M.; Goyal, N.; Du, J.; Joshi, M.; Chen, D.; Levy, O.; Lewis, M.; Zettlemoyer, L.; and Stoyanov, V. 2019. RoBERTa: A Robustly Optimized BERT Pretraining Approach. *arXiv preprint arXiv:1907.11692*.
- Liu, Y.; Xiao, F.; Zhang, Z.; Yu, Y.; Huang, C.; Gao, F.; Wang, X.; Ban, M.-b.; Fan, M.; Tsering, T.; et al. 2025a. TiSpell: A Semi-Masked Methodology for Tibetan Spelling Correction covering Multi-Level Error with Data Augmentation. *arXiv preprint arXiv:2505.08037*.
- Liu, Y.; Yang, B.; Chen, Y.; Zhou, Y.; and He, X. 2023. Multi-level Sentiment-Enhanced Stock Prediction with Hierarchical News Distillation. In *Proceedings of the International Joint Conference on Artificial Intelligence (IJCAI)*, 4376–4382.
- Liu, Y.; Zhang, Z.; Ma-bao, B.; Cai, Y.; Yu, Y.; Duo jie, R.; Wang, X.; Gao, F.; Huang, C.; and Tashi, N. 2025b. FMST-TTS: Few-shot Multi-Speaker Multi-Dialect Text-to-Speech Synthesis for “U-Tsang, Amdo and Kham Speech Dataset Generation. *arXiv preprint arXiv:2505.14351*.
- Loshchilov, I.; and Hutter, F. 2019. Decoupled Weight Decay Regularization. In *ICLR*.
- Ma, Y.; Ma, X.; and Jiang, G. 2025. Insider Trading Patterns During the COVID Period. Working Paper 5163490, SSRN Electronic Journal.
- Mao, A.; Mohri, M.; and Zhong, Y. 2023. Cross-entropy loss functions: Theoretical analysis and applications. In *International conference on Machine learning*, 23803–23828. pmlr.
- Moe, Y. B.; and Ma, Y. 2024. Congressional Stock Trades and Economic Policy Uncertainty. *FEB-RN Research Paper*, (13).
- Montgomery, D. C.; Peck, E. A.; and Vining, G. G. 2012. *Introduction to Linear Regression Analysis*. John Wiley & Sons, 5th edition.
- OpenAI. 2024. GPT-4o Technical Report. <https://openai.com/index/gpt-4o>. Accessed July 2025.
- Pedregosa, F.; Varoquaux, G.; Gramfort, A.; Michel, V.; Thirion, B.; Grisel, O.; Blondel, M.; Prettenhofer, P.; Weiss, R.; Dubourg, V.; Vanderplas, J.; Passos, A.; Cournapeau, D.; Brucher, M.; Perrot, M.; and Duchesnay, É. 2011. Scikit-learn: Machine learning in Python. *Journal of Machine Learning Research*, 12: 2825–2830.
- Reimers, N.; and Gurevych, I. 2019. Sentence-BERT: Sentence Embeddings using Siamese BERT-Networks. *arXiv preprint arXiv:1908.10084*.
- Rumelhart, D. E.; Hinton, G. E.; and Williams, R. J. 1986. Learning representations by back-propagating errors. *Nature*, 323(6088): 533–536.
- Schuster, M.; and Paliwal, K. K. 1997. Bidirectional recurrent neural networks. *IEEE Transactions on Signal Processing*, 45(11): 2673–2681.
- Sutskever, I.; Vinyals, O.; and Le, Q. V. 2014. Sequence to Sequence Learning with Neural Networks. In *Advances in Neural Information Processing Systems*, volume 27.
- Tatsat, H.; and Shater, A. 2025. Beyond the Black Box: Interpretability of LLMs in Finance. *SSRN*.

- Team, Q.; and Cloud, A. 2024a. Qwen-2 Technical Report. *arXiv preprint arXiv:2407.10671*.
- Team, Q.; and Cloud, A. 2024b. Qwen2.5: Open Models with 1-Million Token Context Window. *arXiv preprint arXiv:2412.15115*.
- Team, Q.; and Cloud, A. 2025. Qwen-3 Technical Report. *arXiv preprint arXiv:2505.09388*.
- Team, T. L.; and AI, M. 2024. The LLaMA-3 Herd of Models. In *arXiv preprint arXiv:2407.21783*.
- Touvron, H.; Lavril, T.; Izacard, G.; Martinet, X.; Lachaux, M.-A.; Lacroix, T.; Rozière, B.; Goyal, N.; Hambro, E.; Azhar, F.; Rodriguez, A.; Joulin, A.; Grave, E.; and Lample, G. 2023a. LLaMA: Open and Efficient Foundation Language Models. *arXiv preprint arXiv:2302.13971*.
- Touvron, H.; Martin, L.; Stone, K.; Albert, P.; Almahairi, A.; Babaei, Y.; Bashlykov, S.; Batra, A.; Bhargava, P.; Bhosale, S.; et al. 2023b. LLaMA 2: Open Foundation and Fine-Tuned Chat Models. *arXiv preprint arXiv:2307.09288*.
- Vaswani, A.; Shazeer, N.; Parmar, N.; Uszkoreit, J.; Jones, L.; Gomez, A. N.; Kaiser, Ł.; and Polosukhin, I. 2017. Attention is All You Need. In *Advances in Neural Information Processing Systems*, volume 30.
- Wang, B.; Yao, Y.; Liu, J.; and Zhang, X. 2022. GATSF: Graph Attention Networks for Multivariate Stock Forecasting with Multi-Frequency Price Relations. In *Proceedings of the Conference on Empirical Methods in Natural Language Processing (EMNLP)*, 911–923.
- Wang, H.; Zhang, X.; and Zhao, Y. 2022. Temporal Graph Attention for Stock Movement Prediction with Multi-Source News. In *Proceedings of the Conference on Neural Information Processing Systems (NeurIPS)*.
- Wang, X.; Chi, J.; Tai, Z.; Kwok, T. S. T.; Li, M.; Li, Z.; He, H.; Hua, Y.; Lu, P.; Wang, S.; et al. 2025. Finsage: A multi-aspect rag system for financial filings question answering. *arXiv preprint arXiv:2504.14493*.
- Wang, Y.; Zhang, H.; Feng, Y.; Zhao, C.; and Zhang, W. 2023. FinCLUE: Towards Interpretable Financial Stock Movement Prediction via Contrastive Learning. In *Proceedings of the International Conference on Learning Representations (ICLR)*.
- Wu, Q.; Zhao, W. X.; Chen, Y.; Lian, D.; and Zhang, W. 2022. GRL4Fin: Graph Reinforcement Learning for Financial Portfolio Management. In *Proceedings of the ACM SIGKDD Conference on Knowledge Discovery and Data Mining (KDD)*, 1089–1099.
- Xu, W.; Liu, W.; Xu, C.; Bian, J.; Yin, J.; and Liu, T.-Y. 2021. REST: Relational Event-driven Stock Trend Forecasting. In *Proceedings of The Web Conference (WWW)*.
- Xu, Y.; Wang, H.; and Guo, L. 2021. REST: Relational Stock Ranking with Trading Records. In *Proceedings of the AAAI Conference on Artificial Intelligence*, volume 35, 4463–4470.
- Yang, X.; Cao, C.-Y.; Liu, Y.; Liu, Y.; Wang, L.; Zhang, Q.; Hu, X.; and Zhang, X.-Y. 2023. FinGPT: An Open-Source Large Language Model for Finance. *arXiv preprint arXiv:2306.06031*.
- Yang, Y.; Zhang, X.; and Zhang, Q. 2020. AdaInt: Financial Stock Prediction Using Adaptive Interactions Across Multiple Text Sources. In *Proceedings of the Conference on Empirical Methods in Natural Language Processing (EMNLP)*, 3987–3997.
- Zhang, W.; Chen, Y.; and Zhao, W. X. 2020. Stock Movement Prediction with News-Enhanced Relational Stock Graph. In *Proceedings of the ACM SIGIR Conference on Research and Development in Information Retrieval (SIGIR)*, 1419–1428.
- Zhou, H.; Zhang, S.; Peng, J.; Zhang, S.; Li, J.; Xiong, H.; and Zhang, W. 2021. Informer: Beyond Efficient Transformer for Long Sequence Time-Series Forecasting. In *Proceedings of the AAAI Conference on Artificial Intelligence*, volume 35, 11106–11115.
- Zhou, K.; Li, Z.; Liu, J.; Ding, Z.; Pan, X.; Du, Y.; Yang, H.; Tan, M.; and Zhang, R. 2022. CINO: Cross-Format Information and Numerical Reasoning over Financial Text. In *Proceedings of the 60th Annual Meeting of the Association for Computational Linguistics (ACL)*, 4627–4639. Association for Computational Linguistics.

Supplementary Material

IFD: Statistical Characteristics

The IFD dataset reveals substantial insider activity around sensitive events. Over 56,000 trades are part of stealth sequences, multiple same-direction trades disclosed only after the final transaction. It includes 697 round-trip trades, where insiders reversed positions before reporting. About 43,000 trades occur within 60 days before earnings announcements but are disclosed post-announcement, suggesting misuse of private information. Twenty-one trades occurred during fraudulent restatement periods, with filings delayed by hundreds of days. On average, reporting delays span 37 business days. Intentional purchases are delayed by 116 days, and sales by 77 days. Delinquent purchases average \$457,485 in value; sales, \$1.36 million. These trades earn abnormal returns: late-filed purchases gain 0.03% per day, with total abnormal returns reaching 4.64% during the delay window. The IFD dataset provides a reliable and representative sample for studying insider behavior, information asymmetry, and corporate governance. To ensure data integrity, amended filings were excluded, and only transactions with high-quality flags (R, H, C, L, I) were retained, each indicating trustworthy data from direct filings, manual entry, corrected errors, logical inference, or system-estimated values. Records with report dates before trade dates or implausible volumes were also removed to maintain analytical validity. The data was aggregated at the level of daily transactions per insider, and further classified by buy and sell types. Transactions arising from equity awards or option executions were also eliminated. Additionally, trades with abnormal prices, defined as those deviating more than $\pm 20\%$ from the CRSP closing price, were filtered out. Finally, all financial variables were lagged and subjected to winsorization at the 1st and 99th percentiles to mitigate the influence of outliers.

IFD: Key Parameter

We summarize some key parameters in the IFD dataset. These variables are primarily used to describe the constructed variables, capturing key indicators related to insider trading behavior, violation characteristics, firm financial status, and corporate governance structure.

First, for the insider violation characteristics, Insider Ratio and Firm Ratio reflect the historical violation frequency at the individual and firm levels, providing a measure of the propensity for violations. These variables are extensively used in violation behavior analysis, such as examining the likelihood of violations and reporting delays. For the Insider Ratio, its formula expression is as Eq. 7:

$$InsiderRatio = \frac{Violations}{Trades} \quad (7)$$

where *Violations* means that the historical number of violations by an insider and *Trades* means that the total trades by that insider (dynamically updated). For Firm Ratio, its formula expression is as Eq. 8:

$$FirmRatio = \frac{Violations_Firm}{Trades_Firm} \quad (8)$$

where *Violations_Firm* means that the historical number of violations in a firm and *Trades_Firm* means that the total insider trades within the firm (dynamically updated).

Then, for the trade characteristics and market reactions, Trade Value measures the ratio of trade amount to the firm's market capitalization, which helps assess the impact of trade size on abnormal returns. $\ln(\text{Distance})$ is the Natural log of the distance between the firm's headquarters and the nearest of the 10 largest U.S. metropolitan areas, reflecting information asymmetry and regulatory oversight challenges. For the Trade Value, its formula expression is as Eq. 9:

$$TradeValue = \frac{Trade_Amount}{Market_Cap} \quad (9)$$

where *Trade_Amount* means that the transaction value and *Market_Cap* means that the firm market capitalization. For the $\ln(\text{Distance})$, its formula expression is as Eq. 10:

$$\ln(\text{Distance}) = \ln(\text{Distance}) \quad (10)$$

where *Distance* means that the distance between the firm's headquarters and the nearest of the 10 largest U.S. metropolitan areas. Next, for the corporate governance and ownership structure, Blockholder Ratio and HHI Index capture the concentration of ownership and the influence of blockholders, providing insights into the role of shareholder concentration in mitigating filing violations. These variables are commonly used to analyze the relationship between corporate governance and violation behavior. For the Blockholder Ratio, its formula expression is as Eq. 11:

$$BlockholderRatio = \frac{Shares_Blockholders}{Shares} \quad (11)$$

where *Shares_Blockholders* means that the shares held by Blockholders and *Total_Shares* means that the total shares outstanding. For the HHI Index, its formula expression is as Eq. 12:

$$HHI = \sum_{k=1}^n (Ownership_Share_k)^2 \quad (12)$$

where *HHI Index* is the sum of squared ownership proportions of all observable shareholders (measures concentration) and *k* is the number of all observable shareholders.

Finally, for the firm financial status and growth metrics, ROA, Leverage, B/M, and R&D/Assets describe the firm's operational and financial conditions. These financial variables act as control variables in regression models, helping to assess how firm-level financial environments affect violation behavior. Tobin's Q, as shown in Eq. 13, measures the ratio of market value to the replacement value of assets, enabling the analysis of the long-term impact of filing violations on firm valuation.

$$Tobin'sQ = \frac{Market_Value_of_Firm}{Replacement_Value_of_Assets} \quad (13)$$

For the ROA, Leverage, B/M, R&D/Assets and the Tobin's Q, their formula expressions are as Eq. 14, Eq. 15, Eq. 16 and Eq. 17:

$$ROA = \frac{Net_Income}{Total_Assets} \quad (14)$$

where ROA measures how efficiently a company uses its assets to generate net income. A higher ROA indicates greater efficiency in asset utilization and stronger profitability. It's commonly used to compare performance across companies or over time within the same firm.

$$Leverage = \frac{Total_Liabilities}{Total_Assets} \quad (15)$$

where Leverage indicates the proportion of a company's assets that are financed by debt; a measure of financial risk. A higher leverage ratio means the firm relies more on debt financing, which increases financial risk but can also amplify returns if managed well.

$$B/M = \frac{Book_Value_of_Equity}{Market_Value_of_Equity} \quad (16)$$

where B/M reflects the relationship between a company's book value and its market value. High B/M often considered "value stocks"—undervalued by the market. Low B/M often seen as "growth stocks"—with high market expectations. It is widely used in asset pricing, including in the Fama-French three-factor model.

$$R\&D/Assets = \frac{R\&D_Expenditure}{Total_Assets} \quad (17)$$

where R&D/Assets measures the proportion of total assets devoted to research and development expenditures. A higher ratio suggests that the firm is heavily investing in innovation and future growth. It's especially relevant in tech-intensive or pharmaceutical industries.

In summary, these variables are essential for describing the characteristics of the dataset by capturing trading patterns, insider behavior, governance structures, and financial profiles. They provide a solid empirical foundation for subsequent statistical analysis and theoretical validation.